Joint Input and State Estimation of a Scaled Wind Turbine Model: An Experimental Study

ZIMO ZHU and SONGYE ZHU

ABSTRACT

Structural health monitoring (SHM) has gained recognition in civil engineering and is now a well-established technique. Recently, it has received considerable research attention in the application in Wind turbine (WT) structures. A complete sensing system could provide comprehensive information about the structure during long-term operations. In this study, a 1:50 scaled WT model of the 5-MW reference WT presented by the National Renewable Energy Laboratory (NREL) was designed and manufactured, and a comprehensive SHM sensing system was installed on the WT tower. The system included accelerometers, strain gauges, and as well as a camera system that integrated digital image correlation (DIC) technology and binocular stereo vision technology. By employing the joint input and state estimation (JISE) technique, both the unmonitored structural responses and the unknown interface input were estimated. The study found that blade rotation exerted significant effects on the WT tower responses. The feasibility of WT SHM using the camera system was also validated and discussed in the research. These findings establish a basis for future dynamic analysis of WT structures using the estimated responses and input. Moreover, the study results present a cost-effective approach for monitoring the structural health of WT systems.

Department of Civil and Environmental Engineering, The Hong Kong Polytechnic University, Hong Kong, China

1. INTRODUCTION

Wind energy has experienced significant growth in recent years, as indicated by a substantial increase in annual installations from 6.5 GW in 2001 to 93.1 GW in 2021 [1]. However, the industry faces a significant challenge in the form of high operating and maintenance costs. This challenge is particularly pronounced in the case of offshore wind turbines (OWTs), where wind farms are often located in remote areas to optimize energy production. Consequently, limited accessibility and labor-intensive maintenance processes pose genuine difficulties. Therefore, there is a growing need to explore efficient and cost-effective maintenance strategies as a future trajectory.

SHM has emerged as a well-established technique in civil engineering. By installing sensing systems, the operational status of the structure can be monitored. Recently, SHM has been introduced to the wind industry, leading to the integration of comprehensive sensing systems in numerous WTs, such as [2-4]. These systems commonly adopt various sensor types, such as accelerometers, strain gauges, temperature sensors, GPS, and displacement sensors. The objective of these sensors is to capture and record structural responses, enabling remote assessment of the health condition of WTs under operational conditions.

Compared with the monitoring of structural responses, the direct monitoring of input poses significant challenges, particularly in the case of distributed loads such as wind loads. Budget constraints and the complexities associated with construction often result in limitations on the number and types of available sensors. Consequently, how to obtain structural responses under unknown input with only partial observations has attracted considerable research input. Kalman Filter (KF) based algorithms have gained popularity due to their efficient computational speed and the ability to account for measurement uncertainties. The unknown input and state can be estimated in one single step using Augmented Kalman Filter (AKF) [5]. However, the applicability of AKF-based methods is hindered by the observability problem. An alternative approach involves separately estimating the unknown input and state vector. Gillijns and De Moor proposed two-step optimal, unbiased, and minimum-variance input estimation algorithms [6, 7]. The algorithm, referred to as GDF [7], serves as the foundational framework for many existing JISE algorithms employed in structural dynamics [8].

Despite the significant advancements of JISE algorithms, their application in WTs remains limited. This limitation arises due to the intricate nature of WT structures and the complex excitation mechanisms they are subjected to. To address this gap, the present study designed a 1:50 scaled model based on the 5-MW reference WT presented by the NREL [9]. A comprehensive SHM sensing system was installed on the WT tower. This system comprised accelerometers, strain gauges, and a camera system that integrated DIC technology and binocular stereo vision technology. The estimated structural responses were compared to the measured values in order to assess filter performance.

This paper is organized as follows: First, the presented GDF-based JISE methodology is discussed in Section 2 Methodology. The Section 3 discusses the scaled WT model design and experiment setup in detail. The test results and corresponding discussions are presented in Section 4. Finally, Section 5 concludes the paper by summarizing the key findings derived from this investigation and giving recommendations for future research.

2. METHODOLOGY

This study employs a simplified cantilever beam model to represent the wind turbine tower, thereby facilitating the analysis process. To simplify the calculations, the rotor nacelle assembly (RNA) is treated as a concentrated mass. The impact of the RNA on the wind turbine tower is accounted for through the presence of unknown interface loads $\mathbf{p}(t)$ acting on the tower top. The primary objective of this research is to estimate both the unknown interface loads $\mathbf{p}(t)$ and the structural dynamic responses at unmonitored locations.

JISE algorithms commonly utilize the state space representation (Eqs (1) and (2)) to facilitate iterative processes. The state vector $\mathbf{z}(t)$, comprising the structural displacement and velocity, is instrumental in this representation. The determination of the system matrix $\mathbf{A}_c$ and the input matrix $\mathbf{B}_c$ relies on the structural properties and the location of the unknown input, as described in Eq (3). While the output influence matrix $\mathbf{C}_c$ and the direct feedthrough matric $\mathbf{D}_c$ need also consider the available sensor types and their locations, as denoted by Eq (4).

$$\dot{\mathbf{z}}(t) = \mathbf{A}_c\mathbf{z}(t) + \mathbf{B}_c\mathbf{p}(t), \tag{1}$$

$$\mathbf{y}(t) = \mathbf{C}_c\mathbf{z}(t) + \mathbf{D}_c\mathbf{p}(t). \tag{2}$$

$$\mathbf{A}_c = \begin{bmatrix} \mathbf{0}_{n_{\mathrm{DOF}}} & \mathbf{I}_{n_{\mathrm{DOF}}} \\ -\mathbf{M}^{-1}\mathbf{K} & -\mathbf{M}^{-1}\mathbf{C} \end{bmatrix},\ \mathbf{B}_c = \begin{bmatrix} \mathbf{0}_{n_{\mathrm{DOF}}} \\ \mathbf{M}^{-1}\mathbf{S}_p \end{bmatrix}, \tag{3}$$

$$\mathbf{C}_c = \begin{bmatrix} \mathbf{S}_{\mathrm{str}}\mathbf{B}_{\mathrm{sd}} & \mathbf{0} \\ -\mathbf{S}_{\mathrm{acc}}\mathbf{M}^{-1}\mathbf{K} & -\mathbf{S}_{\mathrm{acc}}\mathbf{M}^{-1}\mathbf{C} \end{bmatrix},\ \mathbf{D}_c = \begin{bmatrix} \mathbf{0} \\ \mathbf{S}_{\mathrm{acc}}\mathbf{M}^{-1}\mathbf{S}_p \end{bmatrix}. \tag{4}$$

Consider a typical scenario in SHM where both acceleration and strain measurements are available. In this case, the observation vector $\mathbf{y}(t)$ can be computed using Eq (5), wherein the selection matrices $\mathbf{S}_{\mathrm{str}}$ and $\mathbf{S}_a$ are determined based on the respective sensor locations. To establish the relationship between displacement and strain, the matrix $\mathbf{B}_{\mathrm{sd}}$ is defined using finite element analysis, facilitating the transmission process.

$$\mathbf{y}(t) = \begin{bmatrix} \mathbf{S}_{\mathrm{str}} & \mathbf{0} \\ \mathbf{0} & \mathbf{S}_a \end{bmatrix} \begin{bmatrix} \mathbf{B}_{\mathrm{sd}}\mathbf{x}(t) \\ \ddot{\mathbf{x}}(t) \end{bmatrix}. \tag{5}$$

The GDF encompasses a three-step design. Beginning with discretizing the state space equation in the time domain, the first step involves estimating the unknown input $\hat{\mathbf{p}}_k$ using Eq (6), where $\mathbf{M}_k$ represents the gain matrix. Then the measurement update of the state vector will be conducted by incorporating the estimated unknown input $\hat{\mathbf{p}}_k$. This update is facilitated by the utilization of the gain matrix $\mathbf{K}_k$, which appropriately balances the predictions and observations. Lastly, the state estimation is propagated to

(a) (b)

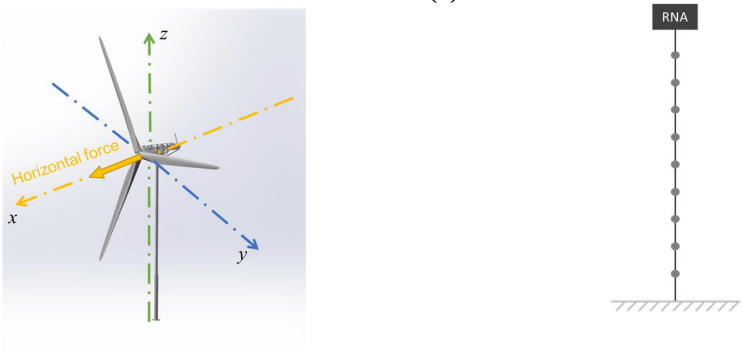

Figure. 1. Decomposition of unknown forces acting on WT tower

the next time step using Eq (8), ensuring the progression of the estimation process in subsequent iterations.

Unknown input estimation

$$\hat{\mathbf{p}}_k = \mathbf{M}_k \left(\mathbf{y}_k - \mathbf{C}_k \hat{\mathbf{z}}_{k|k-1} \right), \tag{6}$$

Measurement update of the state vector

$$\hat{\mathbf{z}}_{k|k} = \hat{\mathbf{z}}_{k|k-1} + \mathbf{K}_k \left(\mathbf{y}_k - \mathbf{C}_k \hat{\mathbf{z}}_{k|k-1} - \mathbf{D}_k \hat{\mathbf{p}}_{k/k} \right), \tag{7}$$

Time update of the state vector

$$\hat{\mathbf{z}}_{k|k+1} = \mathbf{A}_{k-1} \hat{\mathbf{z}}_{k|k} + \mathbf{D}_k \hat{\mathbf{p}}_{k/k} . \tag{8}$$

3. EXPERIMENTAL MODEL AND SETUP

The NREL 5MW reference WT [9] is one of the predominant numerical models utilized in wind energy research. In this study, an experimental model was developed as a 1:50 scaled version of the aforementioned 5MW reference WT [9]. The design of this test model adhered to the geometric scaling principle, with the specific objective of validating the dynamic responses of an onshore WT featuring a fixed bottom design. Notably, the scaled WT blade was also manufactured in accordance with the geometric scaling factor; however, the Reynolds number criteria were not satisfied in this scaled model. As a remedy, a motor was installed within the WT nacelle to drive the blades at varying rotational speeds, thus simulating realistic operating conditions.

As shown in Figure 2, a complete SHM sensing system was installed at the WT tower. This system comprises 11 strain gauges and seven accelerometers. A data acquisition system was employed to sample the sensor data at a rate of 500 Hz. Additionally, to enable non-contact recording of structural displacement, a 3D camera measurement system that integrated DIC technology and binocular stereo vision technology was also incorporated. The frame rate was set at 100 frames per second, and the system achieved a measurement resolution of up to 0.01 pixels by tracking specific

Figure. 2. The scaled WT model and SHM sensing system

markers. In this particular test, 11 markers were deployed to facilitate the extraction of displacements at each node of interest.

Six industrial fans were installed before the WT structure to generate wind excitations. The highest wind speed generated by the fans at the hub height was approximately 3m/s. It should be noted that in the current study, the WT was subjected to combined driving forces originating from both the motor and the wind excitation.

4. RESULTS AND DISCUSSIONS

During the experiment, the blade rotational speed was defined as 90 revolutions per minute (RPM). To replicate real-world operational conditions, the incoming wind excitation was generated by industrial fans. It is worth noting that the wind force exerted on the WT tower can be disregarded due to the relatively small areas involved. Consequently, the focus of the current study lies solely in estimating the interface load between the RNA and the WT tower.

The filter performance was initially assessed by examining the dynamic responses of the structure. The comparison between the estimations obtained through the GDF algorithm and the sensor observations is presented in Figure 3. Both the strain and acceleration estimations exhibit satisfactory agreement with the sensor measurements. However, significant disparities are observed in the results of the displacement reconstruction, as illustrated in Figure 3(c). It was discovered that the displacement observations tracked by the DIC system exhibit periodic peaks. This occurrence can be

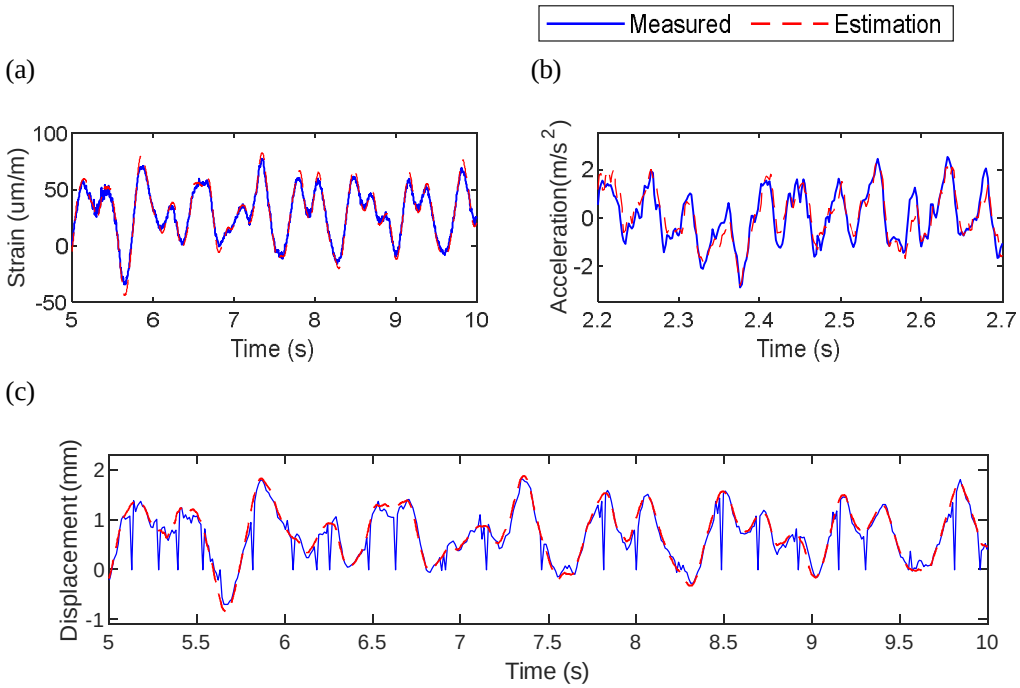

Figure. 3. Dynamic response reconstruction results at element 6 (a) strain; (b) acceleration; and (c) displacement

attributed to implementing binocular stereo vision technology within the DIC camera system, which employs two cameras for 3D measurements. The tested structure should be positioned along the center line of the DIC system as required. Therefore, one of the cameras occasionally became obstructed, resulting in zero readings during the passage of the rotating blades. Consequently, the periodic peaks in the displacements tracked by the DIC system can be attributed to this phenomenon. The time interval between two adjacent peaks corresponds to the blade passing frequency, commonly referred to as the 3P frequency. In the present case, the blade passing frequency was calculated as 4.68 Hz, leading to the determination of the blade rotational speed as 93.6 RPM. These findings indicate that the incoming wind excitation slightly accelerated the rotation of the blades.

Since the WT tower was simplified as a cantilever beam, the rotational angle estimation performance was also checked. Monitoring the rotational angle directly poses notable challenges. However, by evaluating the displacements at both ends of the top element, the secant angle α was calculated, as depicted in Figure 4. It is observed that despite the presence of abnormal peaks attributed to the blade passing, a satisfactory agreement between the measured angle and the estimated angle was observed.

To circumvent the need for calculating complex wind excitation, motor excitation, and blade aerodynamic forces, the estimation of the interface force between the WT tower and the RNA was adopted. However, direct monitoring of the unknown input via the sensing system proved impractical, rendering the measured value unavailable for this section. Figure 5(a) shows the time history of the estimated interface force exerted on the tower top, exhibiting pronounced stochastic behavior attributable to the presence of wind excitations. The Fast Fourier Transform (FFT) analysis of this estimated force

(a) Calculation method

(b) Result

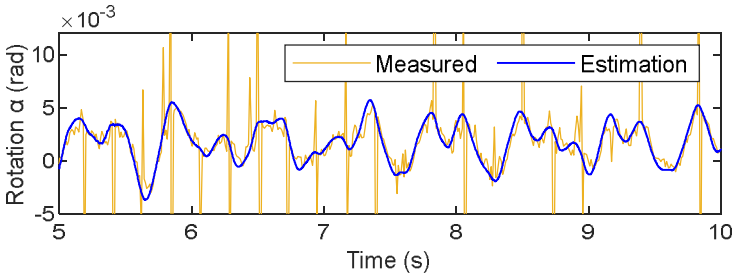

Figure. 4. Rotation angle reconstruction results at element 10

is presented in Figure 5(b), revealing obvious peaks at 0 Hz and 1.56 Hz. The static load component can be ascribed to the steady wind excitation generated by the industrial fans. The frequency of 1.56 Hz corresponds to the predetermined blade rotational speed of 90 RPM. Notice that the actual rotational speed was around 93.6 RPM, indicating a slight acceleration of blade rotation due to the incoming wind. This conclusion aligns with the findings presented in Figure 4.

5. CONCLUSIONS

This experimental study marks the successful validation of JISE for an operational WT. A laboratory test was conducted on a 1:50 scaled model designed according to the NREL 5MW reference WT. The GDF algorithm exhibited sufficient accuracy in estimating both the unknown excitations and unmonitored structural dynamic responses. The findings obtained from this experimental investigation can be summarized as follows:

a) Instead of engaging in complex aerodynamic analysis for direct wind load calculation, a viable and cost-effective alternative lies in employing the KF-based algorithm to reconstruct the unknown interface excitations acting on the tower top.

b) The presented algorithm enables the estimation of structural dynamic responses at unmonitored locations, thereby accommodating applications in partial observation systems.

c) By analyzing the FFT results of the estimated inputs, the rotational speed of the blades can be accurately determined.

The experimental investigations carried out in this study have substantiated the efficacy and resilience of the proposed algorithm. However, the current method is only applicable when the unknown input location has an accelerometer, ensuring compliance with the full rank requirement in the GDF. Additionally, the displacement data tracked through the DIC camera system may exhibit anomalous values. Exploring possible solutions to effectively integrate and fuse these diverse data sources presents a promising avenue for future research.

(a)

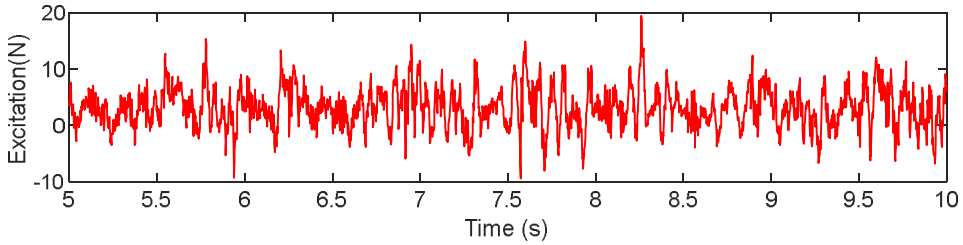

(b)

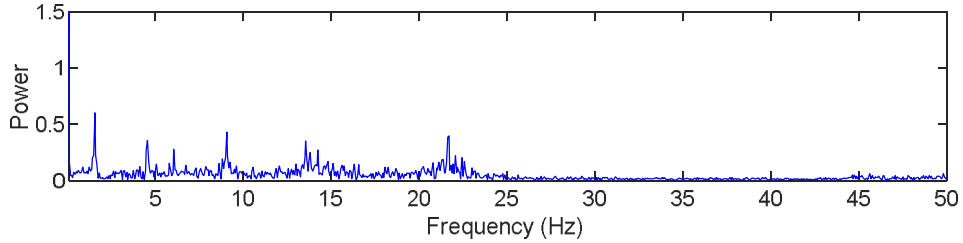

Figure. 5. Reconstructed excitations in time domain (a) force, (b) FFT

REFERENCES

[1] Council, G. W. E. (2022). GWEC Global Wind Report 2022. Global Wind Energy Council: Brussels, Belgium.

[2] Smarsly, K., D. Hartmann, and K.H. Law, An integrated monitoring system for life-cycle management of wind turbines. International Journal of Smart Structures and Systems, 2013. 12(2): p. 209-233.

[3] Veljkovic, M., et al., High-strength tower in steel for wind turbines (HISTWIN). 2012: European Commission Joint Research Centre.

[4] Loraux, C. and E. Brühwiler. The use of long term monitoring data for the extension of the service duration of existing wind turbine support structures. in Journal of Physics: Conference Series. 2016. IOP Publishing.

[5] E. Lourens, E. Reynders, G. De Roeck, G. Degrande, G. Lombaert, An augmented Kalman filter for force identification in structural dynamics, Mech. Syst. Signal Process. 27 (2012) 446–460, https://doi.org/10.1016/j.ymssp.2011.09.025.

[6] S. Gillijns, B. De Moor, Unbiased minimum-variance input and state estimation for linear discrete-time systems, Automatica 43(1) (2007) 111-116. https://doi.org/10.1016/j.automatica.2006.08.002.

[7] S. Gillijns, B. De Moor, Unbiased minimum-variance input and state estimation for linear discrete-time systems with direct feedthrough, Automatica 43(5) (2007) 934-937. https://doi.org/10.1016/j.automatica.2006.11.016.

[8] E. Lourens, C. Papadimitriou, S. Gillijns, E. Reynders, G. De Roeck, G. Lombaert, Joint input-response estimation for structural systems based on reduced-order models and vibration data from a limited number of sensors, Mech Syst Signal Process 29 (2012) 310-327. https://doi.org/10.1016/j.ymssp.2012.01.011.

[9] Jonkman, J., Butterfield, S., Musial, W., & Scott, G. (2009). Definition of a 5-MW reference wind turbine for offshore system development (No. NREL/TP-500-38060). National Renewable Energy Lab.(NREL), Golden, CO (United States).